Analysis of CO2 reduction with micro CHP facility: Renewable energies and Stirling engine

Juan A. Auñon-Hidalgo [1] , Mariano, Sidrach de Cardona [2] Fernando Auñón-Rodríguez [2] and Marta Cordón [3]

[1] Department of Mechanical, thermal and Fluids Engineering. Campus of Teatinos Universidad de Málaga, 29071 (Spain) [2] Department of Applied Phisycs II. E.I.I., Campus of Teatinos Universidad de Málaga, 29071(Spain)
[3] CS Centro Stirling S. Coop, Avda. Álava,3, Aretxabaleta (Gipuzcoa), 20550 Spain

Abstract. The Cogeneration laboratory is a research facility in the University of Málaga (UMA) that allows for the behavioural study of a renewable energy installation combining solar resources and micro-CHP. Energy generation in the system is provided by a 3 kWp photovoltaic array, two solar thermal connectors and a Whispergen EU1 Stirling micro-CHP unit. Energy storage in the facility is provided by water tank and lithium-ion battery. This laboratory is managed through a programmable Mitsubishi PLC that permits the simulation of different thermal and electrical load profiles, as well as the mode of operation. The electrical energy management is controlled by the solar inverter. Environmental data, are measured using a top of the line weather station.The system's real time status is logged through the programmable PLC. All this data is transferred and analysed in a purpose-built MATLAB-based software, where power and energy balances are conducted, efficiencies are calculated, and a CO_2 emissions evaluation is studied.The CO_2 emissions analysis is carried to evaluate the carbon dioxide emissions generated by the facility when the electrical and thermal demand are provided by the joint solar and micro-CHP system. These emissions come from the burning of natural gas in the micro-CHP Stirling engine, and the usage of electricity from the grid. With the current mode of operation, a reduction of up to 70% in CO_2 emissions has been achieved, with an energy generation that exceeds the demand.

1 Introduction

The necessary transition to more sustainable energy systems, in order to combat climate change and its impact on the environment, starts with the reduction in greenhouse gas (GHG) emissions. The burning of fossil fuels for energy to be supplied for electricity, heating, industry and transport accounts for approximately two thirds of the global greenhouse gas emissions.

In this context, one of the six priorities for the European Commission for 2019-2024 is for Europe to be the first climate-neutral continent, through "The European Green Deal" [1]. The European Directive 2018/2001 encourages Member States to take measures to achieve substantial increases in renewable self-consumption, local energy storage and energy efficiency, with a special mention to cogeneration [2].

Some of the key renewable energy technologies are reliant on solar radiation incident on panels (whether photovoltaic or thermal) during daylight. Therefore, there is a need for energy storage to supply for the energy demand during night-time, were solar systems predominant in the energy generation. Moreover, this kind of systems rely on favourable weather conditions to have a sufficient energy yield. Therefore, to apply these technologies in a domestic environment, additional power supplies would be needed to cover for the night demand and adverse weather conditions. Other domestic technologies can be applied for space heating, such as ground source heat pumps [3].

The special mention of cogeneration by policy makers has resulted in the study of new applications for micro-CHP systems that allow for a local power generation (heat and electricity) reducing transport losses and increasing the efficiency. These applications range from the usage of natural gas and biofuels to PV/T systems [4]. Some of the benefits of using Stirling engines are their low wear and long maintenance intervals, compared to other technologies [5], and their almost silent operation. The usage of CHP technologies can improve the operation of renewable power systems, adding flexibility and reducing the

© The Authors, published by EDP Sciences. This is an open access article distributed under the terms of the Creative Commons Attribution License 4.0 (http://creativecommons.org/licenses/by/4.0/).

generation uncertainty [6]. The usage of Stirling engines for micro-cogeneration in the domestic environment is gaining interest, as the literature shows: Conroy et al. [7], Valenti et al. [8] González-Pino et al. [9] Damirchi et al. [10], Grosu et al. [11], Ferreira et al. [12], etc.

Fig. 1. Image of facilities. (On the rooftop and inside the laboratory).

One of the new technologies that is currently being studied is trigeneration, or CCHP: Combined Cooling, Heat and Power. With these systems, both heat and cooling can be provided, as well as electric power. For residential applications, this technology can substantially improve the current implementations of cogeneration, as during roughly half of the year, the thermal heat demand is low —only domestic hot water is needed, but not heat for space heating— with a need for thermal cooling —for space cooling. With CCHP, the heat generated in micro-CHP units can be used for space cooling with the use of an absorption chiller.

After consulting the literature, it has been observed that, although there are analysis on the application of Stirling engine technologies and micro-CHP in domestic applications, there are no other facilities where an experimental system that combines solar energy (through photovoltaic arrays and solar thermal collectors) and micro-CHP with the usage of a Stirling engine is studied. Balcombe et al. [13] simulated the addition of a Stirling engine CHP unit to a solar PV with battery storage system.

2 System description and characteristics

Figure 1 shows images of the installation, with the solar panels (photovoltaic and thermal) on the building rooftop, and the remaining equipment inside the laboratory, whereas Figure 2 shows a diagram of the whole system, where the arrows represent the energy flows in the system (the arrow direction follows the direction of the energy flow)

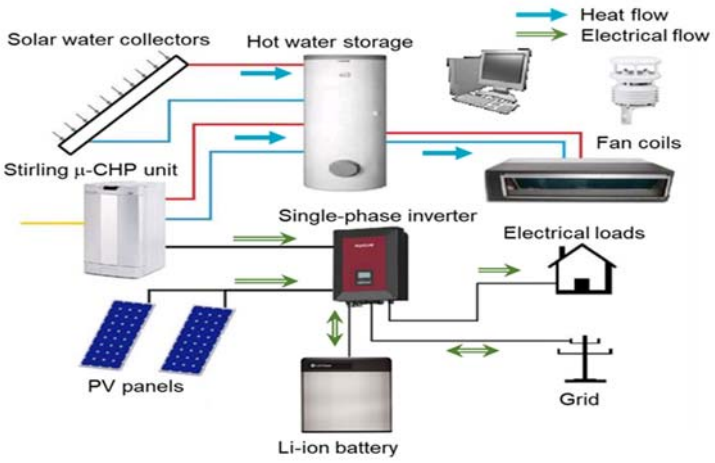

Fig. 2. Diagram of components with energy flow.

The system is divided in two subsystems: an electrical and a thermal subsystem, coupled by the micro-CHP WhisperGen Stirling unit, which generates both heat and electricity. Table 1 shows the different elements installed in the electrical subsystem. This subsystem contains three groups of elements: production, storage and consumption.

Table 1. Component of the electrical subsystem.

Photovoltaic array		**Single phase inverter**		**Battery storage**	
Module Model	Polycrystalline Atersa A-245P	Model	INGECON SUN STO. 1Play 3TL	Model	Li-ion LG 10 kWh
Module Nominal power	245 W	Rated power	3 KVA	Nominal energy	9.8 kWh
Short Circuit current (Isc)	8.82 A	MPPT	1	Nominal capacity	189 Ah
Open circuit voltage (Voc)	37.38 V	Maximum efficiency	95.5 %		
Number of panels	13				

The thermal subsystem contains the equivalent elements as in the electrical one: production, storage and consumption, with water as the working fluid. The heat is generated from two flat plate solar collectors, and the cogeneration unit. Consumption is achieved through two fan coils that can be regulated to follow a thermal load profile. To accommodate for differences in the generation and consumption of thermal energy, a hot water tank is installed, with a capacity of 300 litres. Table 2 shows the main characteristics of the elements in the thermal subsystem.

Table 2. Component of the thermal subsystem.

Solar thermal collectors		**Thermal storage**		**Thermal loads**	
Collector Model	Flat plate Chromagen PA-H	Model	SUICALSA ASF2V-300	Model	Daikin DB_FWE06CT
Fluid capacity	1.2 l	Capacity	300 l	Type	Fan coil
Aperture area	1.87 m²	Power transfer	53 kW	Heating capacity	3.4 /5.63 /6.65 /7.66 kW
Absorber area	1.77 m²			Number of units	2
Total area	2.1 m²				

The Stirling engine micro-CHP unit can produce both heat and electricity, and therefore it is part of both the heat and electricity subsystems. This cogeneration unit has an electrical power of 1 kW, whereas in the thermal output it ranges from 5.5 kW with the main burner and up to 7 kW of thermal output when the auxiliary burner is used to meet the demand requirements.

3 Methodology

The system is running 24/7, the installation is able to apply real thermal and electrical loads according to set demand profiles. Figure 3 shows the electrical and thermal demand curves used in the test, they are typical for a household with peaks of demand in the morning and evening times. Daily total demand of electricity is 17.8 kWh and 7 kWh for thermal.

3.1 Thermal and electrical load profiles

The electrical demand curve (Figure 2) follows the demand profile corresponding to a summer weekday, according to the UK Energy Research Centre (UKERK) datasets [14], with a daily total demand of 17.8 kWh. Due to the fan coils minimum demand limitation the hot water demand (thermal energy) profile (Figure 2) has been adapted from the Spanish institute for the Diversification and Saving of Energy (IDAE), with a total hot water demand of 7 kWh [15], concentrated in two peak demand hours.

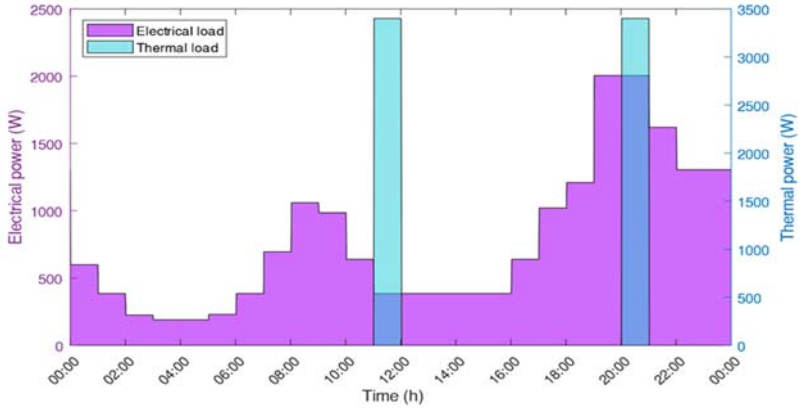

Fig. 3. Electrical and thermal demand curves used in the tests.

3.2 Data analysis

An ad hoc software application has been developed using the computing power provided by MATLAB® to be able to both analyse and visualize the most relevant information during the tests. After the analysis is run, the software displays all the results in numerical data, tables and plots, to be able to study the evolution of the system in the most convenient and intuitive way. An example of electrical analysis by this software is showed in Figure 4, in this case regarding the power and energy balance in the electrical subsystem.

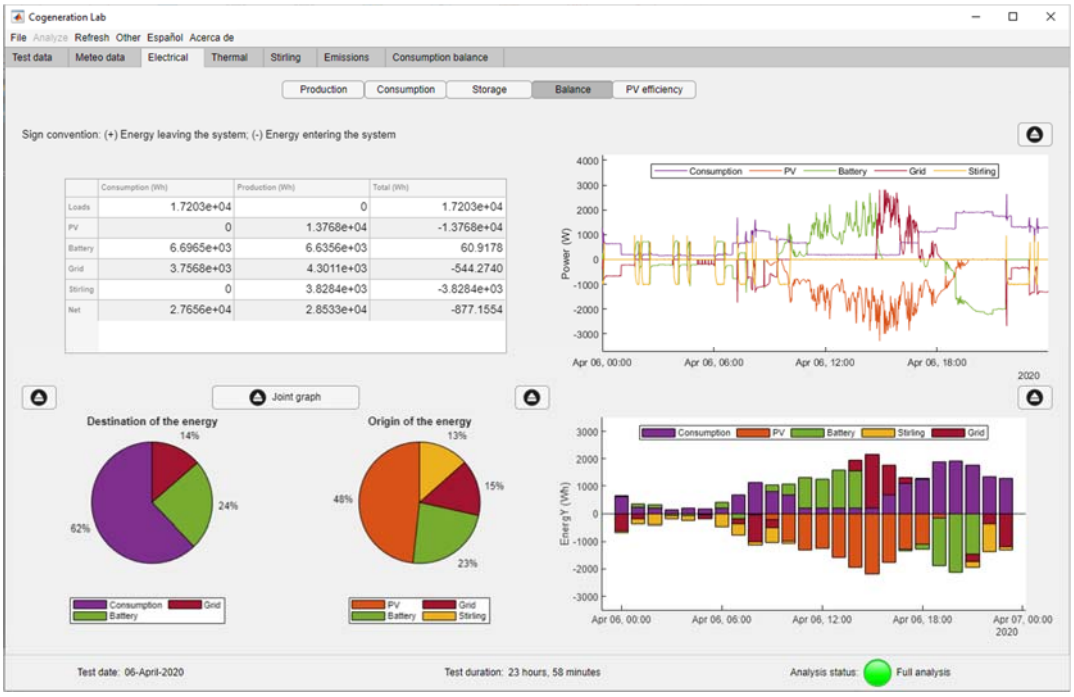

Fig. 4. Screenshot of the analysis and visualization software. The image shows the electrical balance in the system during a 24-hour test.

3.2.1 Electrical parameters

For the electrical analysis, the following efficiency parameters are defined:

* System efficiency or Yield: defined, for a set time period, as the ratio between the energy produced by the system and the peak installed power, expressed in kWh/kWp.

$$Yield\ \left[\frac{kWh}{KWp}\right] = \frac{E_{PV}}{P_{peak}} \quad (1)$$

Where,

E_{PV}, is the energy produced by the PV system.

P_{peak}, is the peak installed power in the PV system.

* Performance Ratio (PR): The Performance Ratio is other parameter to determine the system's quality. This ratio evaluates the overall losses –expressed in %– in the photovoltaic system compared to an ideal system operation, where the installation is supposed to work at STC conditions [16].

$$PR\ [\%] = \frac{E_{PV}}{E_{PV,ideal}} \cdot 100 \quad (2)$$

With

$$E_{PV,ideal} = E_{solar} \cdot \eta_{STC} \quad (3)$$

Where,

$E_{PV,ideal}$, is the ideal energy generated in the system without losses.

E_{solar}, is the received solar energy (Irradiance).

η_{STC}, is the system's efficiency at STC conditions.

The performance ratio and yield are related by the following expression:

$$PR\ [\%] = \frac{Yield}{Y_{ref}} \cdot 100 = \frac{Yield}{\frac{E_{solar}}{1000}} \cdot 100 \quad (4)$$

Where,

Y_{ref}, is the reference Yield, the ratio between the received solar irradiance and the irradiance at STC conditions (1000 W/m²).

In addition to these efficiency definitions, to evaluate this type of photovoltaic installations, these parameters are particularly useful [17]:

- Direct PV Self-consumption (SC_d): Photovoltaic direct self-consumption percentage is defined as the ratio between the energy consumed directly from photovoltaic ($E_{PV,LOAD}$) and the total energy produced by the PV system ($E_{PV,LOAD}$).

$$SC_d\ [\%] = \frac{E_{PV,LOAD}}{E_{PV}} \cdot 100 \quad (5)$$

- Global PV Self-consumption (SC_g): Global photovoltaic self-consumption percentage is as the ratio between the energy consumed directly from photovoltaic ($E_{PV,LOAD}$) and the energy produced by the PV array used to charge the battery.

$$SC_g\ [\%] = \frac{E_{PV,BAT} + E_{PV,LOAD}}{E_{PV}} \cdot 100 \quad (6)$$

Where

$E_{PV,BAT}$, is the energy produced by the PV array used to charge the battery.

$E_{PV,LOAD}$, is the energy produced by the PV array directly used to meet the system load.

E_{PV}, is the total energy produced by the PV system.

● PV Self-sufficiency: the energy ratio between the PV solar generation directly used in the building and the total building energy consumption, in %, which represents the percentage of electric consumption which is covered by the photovoltaic system.

$$SS\ [\%] = \frac{E_{PV,BAT} + E_{PV,LOAD}}{E_{LOAD}} \cdot 100 \quad (7)$$

Where,

E_{LOAD}, is the total electrical energy consumed in the installation.

3.2.2 Thermal parameters

In addition to the energy balances, the following ratios are defined:

- Useful heat ratio: defined as the percentage of thermal energy in the system that has been dissipated due to the thermal storage being at its maximum operating temperature in relation to the total thermal energy consumed in the system (either dissipated or being used to meet the thermal demand).

$$HR\ [\%] = \frac{E_{heat,dissipated}}{E_{heat,load} + E_{heat,dissipated}} \cdot 100 \quad (8)$$

Where,

$E_{heat,dissipated}$, is the thermal energy dissipated in the system.

$E_{heat,load}$, is the thermal energy consumed to meet thermal loads.

- Theoretical solar coverage: defined as the ratio between the solar thermal generation and the thermal demand. It expresses the amount of the daily demand that could have been supplied by the solar heat collectors.

$$TSC\ [\%] = \frac{E_{Solar,heat}}{E_{heat,demand}} \cdot 100 \quad (9)$$

Where,

$E_{Solar,heat}$, is the thermal energy generated in the solar heat collectors.

$E_{heat,demand}$, is the thermal demand of the system.

- Real solar production ratio: defined as the ratio between the solar thermal generation and the total thermal consumption.

$$SP\ [\%] = \frac{E_{Solar,heat}}{E_{heat,TOTAL}} \cdot 100 \quad (10)$$

Where,

$E_{Solar,heat}$, is the thermal energy generated in the solar heat collectors.

$E_{heat,TOTAL}$, is the total thermal consumption of the system, including the demand and the dissipated heat.

- Real Stirling production ratio: defined as the ratio between the Stirling engine thermal generation and the total thermal consumption.

$$SP\ [\%] = \frac{E_{Stirling,heat}}{E_{heat,TOTAL}} \cdot 100 \quad (11)$$

Where,

$E_{Stirling,heat}$, is the thermal energy generated in the Stirling engine.

$E_{heat,TOTAL}$, is the total thermal consumption of the system, including the demand and the dissipated heat.

3.2.3 Stirling parameters

The efficiency of the unit is obtained globally and the generator's efficiency in the thermal and electrical production:

- Stirling global efficiency: defined as the ratio between the total energy produced by the Stirling engine and the energy of the burnt natural gas to generate it.

$$\eta_{stirling}\ [\%] = \frac{E_{Stirling,el} + E_{Stirling,th}}{E_{NG}} \cdot 100 \quad (12)$$

Where,

$E_{Stirling,el}$, is the electrical energy generated in the Stirling unit.

$E_{Stirling,th}$, is the thermal energy generated in the Stirling unit.

E_{NG}, is the energy produced by the combustion of the natural gas.

- Stirling electrical efficiency: defined as the ratio between the electricity produced by the Stirling engine and the energy of the burnt natural gas to generate it.

$$\eta_{stirling,el}\ [\%] = \frac{E_{Stirling,el}}{E_{NG}} \cdot 100 \quad (13)$$

Where,

$E_{Stirling,el}$, is the electrical energy generated in the Stirling unit.

E_{NG}, is the energy produced by the combustion of the natural gas.

- Stirling thermal efficiency: defined as the ratio between the heat produced by the Stirling engine and the energy of the burnt natural gas to generate it.

$$\eta_{stirling,th}\ [\%] = \frac{E_{Stirling,th}}{E_{NG}} \cdot 100 \quad (14)$$

Where,

$E_{Stirling,th}$, is the thermal energy generated in the Stirling unit.

E_{NG}, is the energy produced by the combustion of the natural gas.

3.2.3 CO_2 emissions analysis

The CO_2 emissions generated during the testing have been determined, being divided in the CO_2 emissions associated to the consumption of electrical energy and thermal energy:

- Electrical CO_2 emissions: computed as the CO_2 emissions of the electricity used to meet the electrical loads in the system, they are obtained from the electricity used from the grid ($E_{grid,LOAD}$) with the CO_2 emissions from the electrical mix and the electricity used from the Stirling Engine Unit through its efficiency ($\eta_{stirling}$) and the emissions from the combustion of its fuel, natural gas ($CO_{2,NG}$).

$$CO_{2,el} = E_{grid,LOAD} \cdot CO_{2,grid} + \frac{E_{el,stirling,LOAD} + E_{el,stirling,BATTERY}}{\eta_{stirling}} \cdot CO_{2,NG} \quad (15)$$

Where,

$E_{grid,LOAD}$, is the energy imported from the electrical grid to meet the loads.

$E_{el,stirling,LOAD}$, is the electrical energy from the Stirling used to directly meet the loads.

$E_{el,stirling,BATTERY}$, is the electrical energy from the Stirling used to charge the batteries.

$CO_{2,grid}$, are the specific emissions associated to the electric mix, in kg CO_2/kWh.

$CO_{2,NG}$, are the specific emissions associated to the combustion of natural gas, in kg CO_2/kWh.

$\eta_{stirling}$ is the global efficiency of the Stirling Engine unit.

- Thermal CO_2 emissions: similarly to the electrical CO_2 emissions, the thermal emissions are obtained from the emissions generated by the combustion of natural gas in the Stirling unit to generate the thermal energy used to heat the storage tank and meet the demand load.

$$CO_{2,th} = \frac{E_{th,stirling,LOAD} + E_{th,stirling,STORAGE}}{\eta_{stirling}} \cdot CO_{2,NG} \quad (16)$$

Where,

$E_{th,stirling,LOAD}$, is the thermal energy from the Stirling used to directly meet the loads.

$E_{th,stirling,STORAGE}$, is the thermal energy from the Stirling used to heat the hot water storage.

$CO2_{,NG}$, are the specific emissions associated to the combustion of natural gas, in kg CO_2/kWh.

$\eta_{stirling}$ is the global efficiency of the Stirling Engine unit.

The theoretical emissions in the system are obtained from the thermal and electrical energy consumed in the system:

- Theoretical electrical CO_2 emissions: obtained considering that all the electric demand has been met with energy from the grid.

$$CO_{2,theor,el} = E_{el,LOAD} \cdot CO_{2,grid} \quad (17)$$

Where,

$E_{el,LOAD}$, is the electrical energy consumed in the system.

$CO_{2,grid}$, are the specific emissions associated to the electric mix, in kg CO_2/kWh.

- Theoretical thermal CO_2 emissions: computed as if all the heat consumed in the installation came from a traditional hot water boiler using different sources of energy – natural gas, electricity

$$CO_{2,theor,th} = \frac{E_{th,LOAD}}{\eta_{boiler}} \cdot CO_{2,source} \quad (18)$$

Where,

$E_{th,stirling,LOAD}$, is the thermal energy consumed in the system.

$CO_{2,source}$, are the specific emissions associated either to the combustion of the studied fuel or the use of electricity from the grid, in kg CO_2/kWh.

η_{boiler}, is the seasonal efficiency of the studied boiler (85%).

For the CO_2 emissions factors associated to each energy source, the values published for 2018 by the Ministry for the Energy Transition of Spain [18] have been considered, as well as those published by the Spanish Electricity Network, taking into account the electricity generation mix of Spain for the year 2018 [19]. These values are shown in table 3.

Table 3. Emissions factors associated to each studied energy source [18,19].

Energy source	CO_2 emissions (kg CO_2/kWh)
Natural Gas	0.203
Electric grid	0.246
Diesel oil	0.267

4 Results

The analysis described above has evaluated the results for 18 days between March 29th, 2020 and April 16th, 2020. This selection of days covers a variety of weather conditions in spring, with sunny days, overcast days and rainy days. Therefore, this selection of dates represents a significant period to evaluate the installation across a range of different conditions. Table 4 shows the daily average, maximum and minimum values for the main operating parameters in the system, as well as the standard deviation of these values.

Table 4. Global daily average results from the system testing.

	Average	Maximum	Minimum	STD
Meteorological Parameters				
Solar irradiation (kWh/m²)	4.3	7.3	1.4	2.0
Ambient temperature (ºC)	14.9	16.6	12.5	1.1
Wind speed (m/s)	2.3	4.3	1.2	0.8
Electrical Parameters				
Real Load (kWh)	17.2	17.3	16.6	0.1
Photovoltaic production (kWh)	11.7	20.6	3.3	5.8
Yield (kWh/kWp)	3.9	6.9	1.1	1.9
Performance Ratio (%)	88.4	93.9	79.5	4.0
Direct photovoltaic self-consumption (%)	34.6	55.3	23.1	9.9
Global photovoltaic self-consumption (%)	78.4	99.4	51.1	19.4
Photovoltaic Self-sufficiency (%)	47.4	61.2	18.7	14.0
Stirling electrical production (kWh)	3.8	4.9	2.3	0.6
Grid to load (kWh)	5.9	10.3	3.7	2.1
Thermal Parameters				
Thermal demand (kWh)	6.8	6.8	6.8	0.0
Total heat consumption (kWh)	26.5	31.9	13.0	4.2
Solar heat production (kWh)	1.8	4.1	0.0	1.7
Stirling heat production (kWh)	27.9	35.6	16.2	4.5
Dissipated heat (kWh)	19.5	26.6	5.7	4.2
Useful heat (%)	27.4	56.0	17.0	8.1
Theoretical solar coverage (%)	26.0	60.9	0.0	24.6
Real solar production (%)	6.0	16.6	0.0	5.7
Real Stirling production (%)	94.0	100.0	83.4	5.7
Stirling Engine Performance				
Stirling engine global efficiency (%)	68.4	71.3	66.1	1.4
Stirling engine electrical efficiency (%)	8.2	8.6	7.7	0.2
Stirling engine thermal efficiency (%)	60.2	63.0	58.2	1.2

The climatic parameters show good levels of irradiance and ambient temperature during the testing, with a daily average solar irradiation of 4.3 kWh/m². During the analysed period, the PV system has shown a reliable behaviour, following the maximum power point of the modules, obtaining an average performance ratio of 88.4 %, and a maximum PR of 93.9 %. This high value is possible thanks to a daily average cell temperature of 15.6 ºC, which is better than STC conditions. Under these conditions, 78.4 % of the PV energy generated has been used by the system, reaching a coverage of electricity demand by photovoltaic of 47.4 %.

4.1 Electrical evaluation

Figure 5 shows the daily average photovoltaic generation balance. From the total PV production, 70.3 % was used in the facility, whereas the remaining 29.8 % was injected to the electrical grid. Part of the electricity used in the system was used to charge the batteries (39.6 %), and 30.7 % was used to directly meet the electrical demand.

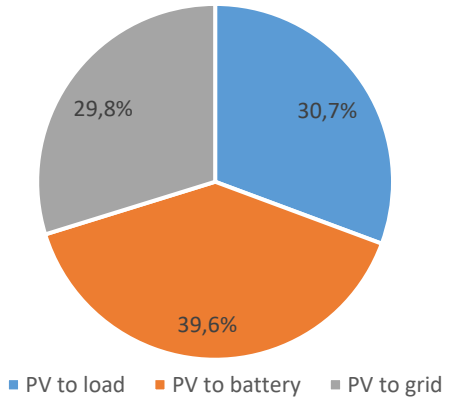

Fig. 5. Energy balance for the daily average photovoltaic generation.

In Figure 6, the daily average energy balance in the electrical subsystem is evaluated, from the load coverage perspective. The PV array provided 45.5 % of the electricity demand, with 19.9 % being supplied directly to the loads, and 25.6 % from the energy used to charge the battery. The Stirling Engine unit generation accounts for 21.3 % of the demand, with 14.6 % of the electricity flowing directly to the load and 6.7 % from the battery charge obtained with its operation. Finally, the remaining 33.2 % of the demand was supplied by the electric grid, as the system could not provide for the required electricity at that time.

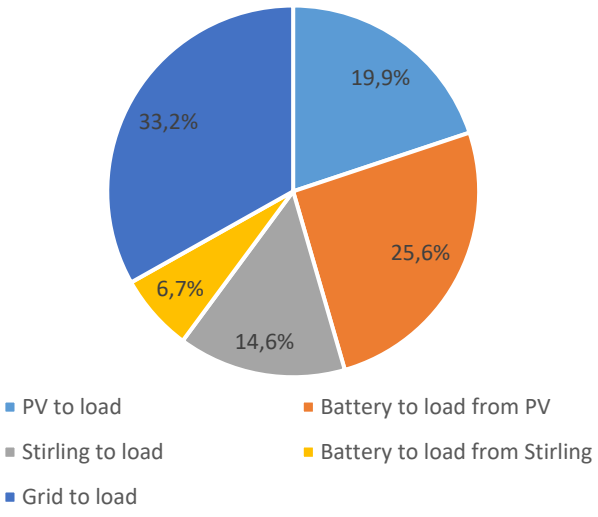

Fig. 6. Daily energy average for the electrical load coverage.

The average amount of electricity injected to the grid (5.9 kWh/day) is higher than the average electricity required from the grid (4.6 kWh/day). Therefore, the system has a net positive electric balance, with more energy generated in the system through sustainable means than the required energy from less sustainable sources.

Figure 7 shows the daily percentages of global PV self-consumption and self-sufficiency as a function of daily irradiation. The results show that, although there is an average electrical global PV self-consumption rate of 78.4 %, for values of daily irradiation up to 3600 Wh/m², it reaches values near 100 %. However, with higher irradiations, it shows an inverse linear behaviour. Considering the self-sufficiency, it linearly increases with the irradiance, and it saturates at 4000 Wh/m² with a self-sufficiency of 60 %.

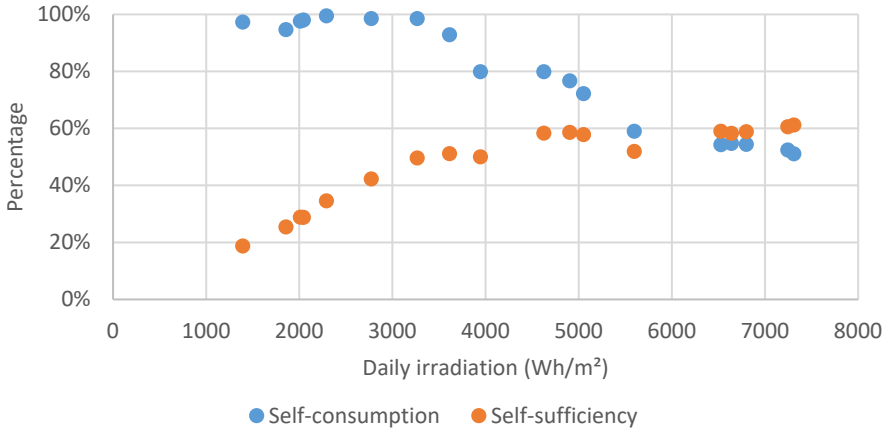

Fig. 7. Daily percentages of global PV self-consumption and PV self-sufficiency as a function of daily irradiation.

The global photovoltaic efficiency (GPE) evaluates the global operation of the photovoltaic system. In Figure 8, this parameter is studied against the photovoltaic production, normalized to the battery capacity. The maximum point in the GPE shows the best operation point in the system. The highest obtained efficiencies are reached when the production is roughly equal to the storage capacity. At that point, the system can take advantage of 95 % of the produced PV energy, with a load coverage of 50 %.

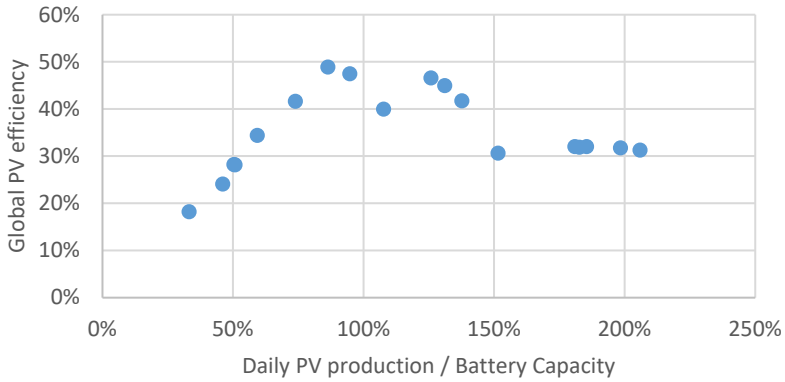

Fig. 8. Daily percentages of global PV self-consumption and PV self-sufficiency as a function of daily irradiation.

With the obtained results, and with the required electricity from the grid during night hour, there is a clear imbalance between the installed PV capacity and the available electric storage. This fact is worsened when considering that the Stirling Engine unit can also charge the electric battery, therefore reducing the available storage for the PV energy. To improve the PV energy usage, the electric storage capacity should be increased, or the generation capacity should be reduced.

4.2 Thermal evaluation

Considering the thermal performance of the system, in Figure 9 the daily average thermal usage is shown. From the total consumption of the thermal subsystem, only 26.4 % of the energy was destined to supply for the thermal demand. The remaining 73.6 % of the heat was dissipated in order to reduce the heat storage temperature at moments where the temperature was above 70 ºC.

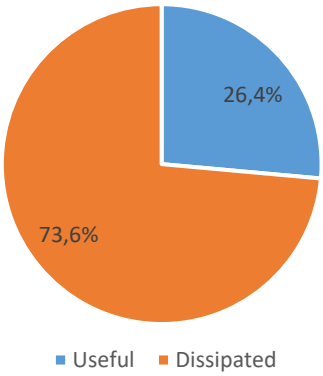

Fig. 9. Daily average of the thermal energy usage in the system.

All the Stirling Unit operation has been to meet the electrical demand during night-time. As it generated electricity, it also produced an average of 27.9 kWh daily. The solar collectors yielded an average of 1.8 kWh each day, which is lower than the thermal demand of the installation. A daily energy production balance for the thermal subsystem is shown in Figure 10. The results show how the Stirling Engine is the primary heat source in the system, accounting for an average of 94 % of the production. The solar thermal collectors produced up to 16.6 % of the total heat generation, with an average of 6 % of the heat generated.

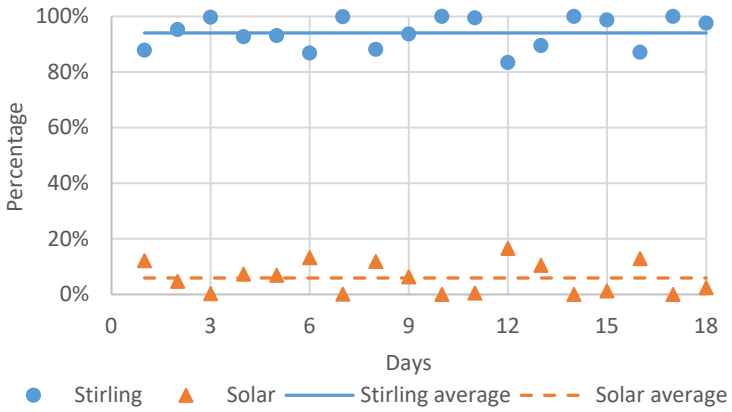

Fig. 10. Heat generation balance for the analysed days.

The low solar heat generation is caused by the lack of synchronization between the heat demand curve and the solar heat production. This fact, added to the high amount of heat generated with the Stirling Engine, which causes the heat storage tank to be at high temperatures, results in the 73.6 % of the heat generated in the system being dissipated.

The current demand curves applied to the system only cover the Domestic Hot Water demand for the household. With the amount of excess heat available, the system could also meet the space heating requirements of the installation. Considering that the space heating requirements are higher at night, which are the times that the Stirling Engine unit is operational to supply the electrical demand, the additional heat demand should improve the heat usage in the system and the synchronization between thermal and electrical demand (which is optimal for the Stirling Engine).

In Figure 11, the theoretical solar coverage is shown for the 18 analysed days. The graph shows the percentage of the useful heat demand that could have been provided by the solar heat collectors. The

average solar coverage is 26 %, reaching a maximum of 60.9 %. However, the solar coverage shows a high variability, where most of the days it is either close to the maximum, or it is near zero.

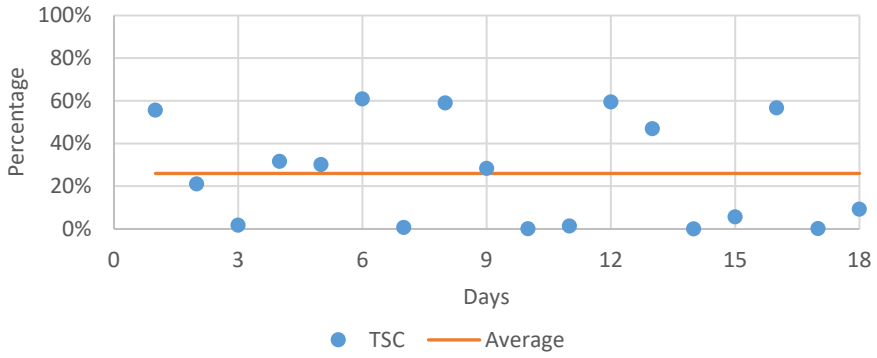

Fig. 11. Theoretical solar coverage for the studied days.

The solar heat collectors are not enough to provide for the heat demand in the installation. The main advantage of the proposed solution –the usage of a Stirling Engine cogeneration unit– is that the unit produces both heat and electricity for the system demand with high efficiency values. As the unit starts to meet the electrical needs, heat is generated and stored in the hot water tank, which is later used to meet the thermal demand.

To increase the heat usage in the installation, the heat storage capacity can be increased to reduce the dissipated heat. However, the ideal solution would be to increase the heat demand, which could be done with the addition of the space heating requirements of the household for colder locations, or with the implementation of trigeneration (CCHP) with an absorption cooling system that could meet the space cooling needs of the household.

4.3 CO_2 emissions analysis

The obtained results for the CO_2 emissions analysis are presented in Table 5. The table shows the real CO_2 emissions of the system, and the theoretical emissions generated in a system where the electricity was provided by the electrical grid and the heat would be generated in a conventional boiler, powered by natural gas, electricity, or diesel oil. The analysis has been conducted considering the energy consumption of the system.

Table 5. Average, maximum, minimum and std values for the daily CO_2 emissions analysis.

	Average	Maximum	Minimum	STD
Real emissions				
Real electrical emissions	2.60	3.77	2.02	0.57
Real thermal emissions	1.68	2.65	1.17	0.46
Real total emissions	4.28	6.14	3.35	0.98
Theoretical emissions				
Theoretical electrical emissions	4.22	4.25	4.10	0.03
Theoretical thermal emissions (natural gas)	1.67	2.14	1.19	0.24
Theoretical thermal emissions (electricity)	2.02	2.60	1.44	0.30
Theoretical thermal emissions (diesel oil)	2.20	2.82	1.56	0.32
Theoretical total emissions (natural gas)	5.89	6.37	5.43	0.25
Theoretical total emissions (electricity)	6.25	6.82	5.68	0.30
Theoretical total emissions (diesel oil)	6.42	7.05	5.80	0.33

During the analysed period, the system has shown average emissions of 4.28 kg CO_2 per day, being the emissions associated to the electrical consumption 60.7 % of the total emissions. Compared to the theoretical emissions, a reduction in CO_2 emissions has been achieved irrespective to the considered source for the heat generation.

Figure 12 reflects the real emissions (first column) compared to the three considered theoretical scenarios. While the increase in the thermal emissions for all the theoretical scenarios (compared to the real emissions) is minimal –due to the high usage of the heat generated in the Stirling unit, and low solar heat usage–, a reduction of 38.4 % in CO_2 emissions has been achieved for the electrical system in comparison with the equivalent amount of electricity used exclusively from the grid.

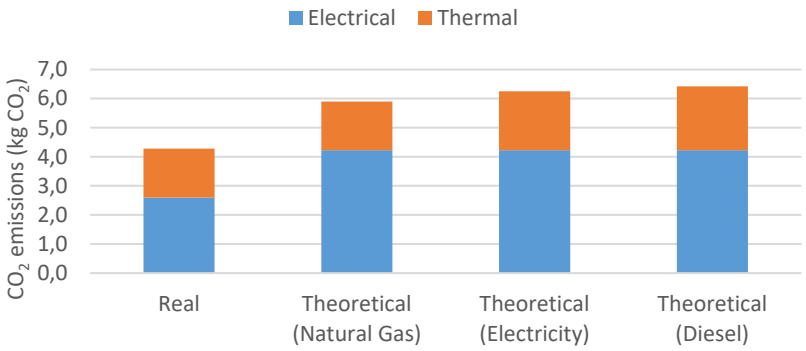

Fig. 12. Average values for the CO_2 emissions analysis.

The total CO_2 emissions obtained (4.28 kg CO_2) are slightly higher than the theoretical electrical emissions (4.22 kg CO_2) showing that the proposed system could provide for both the thermal and electrical needs of a household with practically the same emissions that would be generated to supply for only the electrical demand in a reference household. Considering the total reduction in CO_2 emissions, the generated emissions are up to 33.4 % lower than the total emissions generated in a system using the grid and a diesel oil boiler.

One step to further reduce the real CO_2 emissions in the system would be to increase the electrical storage capacity. This way, and as previously discussed, the PV energy usage would increase and the energetic demand from either the cogeneration unit or the electrical grid would be reduced.

In order to reduce the associated emissions of the Stirling Engine unit, its operational efficiency can be increased. In Figure 13, the electrical and thermal efficiencies of the unit are shown. The electrical efficiency remains constant during all the tests. However, the thermal efficiency fluctuates in the different tests, which caused the total efficiency to vary between days. The source of these variations is the intermittent operation of the unit, which causes long periods of transient thermal behaviour (in the heating and cooling phases), which reduce the efficiency. Under ideal steady conditions, the unit has shown global efficiencies of up to 96.9 %, with an average global efficiency of 86.2 %. Therefore, the CO_2 emissions generated in the Stirling Engine unit could be reduced with a control strategy that minimizes the starts and stops of the unit during the tests.

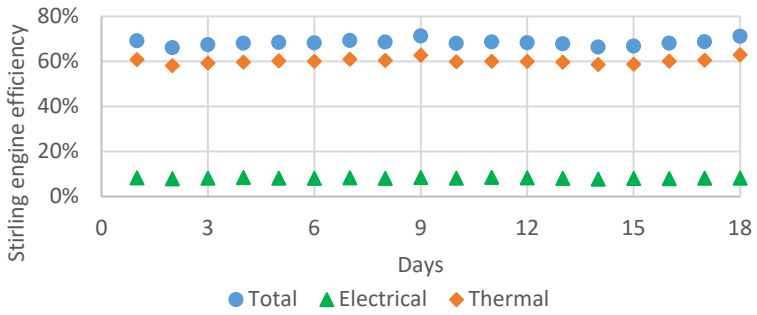

Fig. 13. Stirling Engine global, thermal and electrical efficiencies during the analysed period.

The usage of electricity from the grid adds the grid generation mix to the elements that affect the CO_2 emissions in the system. An average of 33.2 % of the energy consumed in the system was provided by the grid. Thus, the location of the installation will affect the total generated emissions.

5 CONCLUSIONS

This work presents the first experimental results from the joint operation of a novel installation. The system has an EHE WhisperGen Stirling Engine micro-CHP unit and both PV and solar thermal collector arrays. The main objective of the system is to meet all the energetic needs –both thermal and electrical– in an isolated household. To achieve this objective, the energy production and storage, and the synchronization between the energy production and consumption profiles.

The total energy consumption of the evaluated household was 24 kWh, where 71.7 % was correspondent to the electrical demand and the remaining 28.3 % to the thermal demand. The irradiance levels in the analysed days range from 1.4 to 7.3 kWh/m², allowing for the evaluation of the system under a wide spectrum of meteorological conditions.

The photovoltaic system has covered 47.4 % of the daily electrical demand, with a global self-sufficiency of 78.4 %, an average daily performance ratio of 88.4 %, and an average daily yield of 3.9 kWh/kWp. Although there is excess electricity (there was energy exported to the grid), the system required to import electricity during the nights to meet the demand. This fact shows that the battery capacity is low.

Considering the electricity generated in the Stirling Engine unit, the installation has been able to provide 66.8 % of the daily electrical demand, with 21.3 % covered by the Stirling Engine. In the thermal subsystem, the whole energy demand has been provided by the system, with an excess of 73.6 % in heat capacity.

The Stirling Engine unit has shown a high global efficiency (68.4 %), thanks to its ability to generate heat and electricity simultaneously. However, with longer periods of operation, the efficiency can reach up to 86.2 %, and up to 93.9 % under optimal operational conditions.

The electrical coverage of the system has been low, especially during the nights. This was caused by a shortage of storage capacity, and the poor coupling between the electrical generation and demand curves. All the micro-CHP Stirling Engine starts have been to meet the electrical demand, which generated enough heat to meet all the requirements in the household, and it could also meet space heating and/or cooling needs. With higher electric storage capacity, the system could cover a higher percentage of the electric demand.

As a whole, with the current configuration 75.3 % of the total energy demand has been covered. Thanks to the Stirling Engine unit, the whole thermal demand has been met, and its operation was key to supply the thermal energy in the system for low irradiance days.

The system's electrical reliability is improved by the Stirling Engine electrical production during night-time. The obtained results show the importance of the correct energy storage sizing. Doubling the actual battery capacity, reaching 20 kWh of electric storage, would allow the system to cover the complete electrical demand, with one day of electric autonomy. With the increase in electric energy storage capacity, the system could be fully autonomous, and it could be able to cover an additional thermal load of up to 30 kWh either in space heating or air conditioning.

The proposed system achieved a 33.4 % reduction in the CO2 emissions, comparing it with a traditional installation that uses the electricity from the grid and the heat generated in a conventional diesel oil boiler. When analysing the emissions associated to the electricity usage, a reduction of 38.5 % has been achieved.

In future research, the following actions will be taken: an evaluation of the proposed installation with different demand curves and under different radiation conditions; the development of different control strategies to optimize the system and improve the electrical independence from the grid; an upgrade to a

trigeneration system with an absorption chiller, and the evaluation of the sustainability of the system with different energy sources, such as biogas or biomass.

References

1. Von Der Leyen U. Political guidelines of the Commission 2019-2024. (2019).

2. DIRECTIVES DIRECTIVE (EU) 2018/2001 OF THE EUROPEAN PARLIAMENT AND OF THE COUNCIL of 11 December 2018 on the promotion of the use of energy from renewable sources (recast) (Text with EEA relevance). (2018).

3. Esen H, Inalli M, Esen M. A techno-economic comparison of ground-coupled and air-coupled heat pump system for space cooling. *Build Environ* (2007). https://doi.org/10.1016/j.buildenv.2006.04.007.

4. Martinez S, Michaux G, Salagnac P, Bouvier J-L. Micro-combined heat and power systems (micro-CHP) based on renewable energy sources. *Energy Convers Manag* (2017). https://doi.org/10.1016/J.ENCONMAN.2017.10.035.

5. Onovwiona HI, Ugursal VI. Residential cogeneration systems: review of the current technology. *Renew Sustain Energy Rev* (2006). https://doi.org/10.1016/j.rser.2004.07.005.

6. Bagherian MA, Mehranzamir K. A comprehensive review on renewable energy integration for combined heat and power production. *Energy Convers Manag* (2020). https://doi.org/10.1016/j.enconman.2020.113454.

7. Conroy G, Duffy A, Ayompe LM. Economic, energy and GHG emissions performance evaluation of a WhisperGen Mk IV Stirling engine μ-CHP unit in a domestic dwelling. *Energy Convers Manag* (2014). https://doi.org/10.1016/j.enconman.2014.02.002.

8. Valenti G, Campanari S, Silva P, Ravidà A, Macchi E, Bischi A. On-off Cyclic Testing of a Micro-cogeneration Stirling Unit. *Energy Procedia*, (2015). https://doi.org/10.1016/j.egypro.2015.07.152.

9. González-Pino I, Pérez-Iribarren E, Campos-Celador A, Terés-Zubiaga J, Las-Heras-Casas J. Modelling and experimental characterization of a Stirling engine-based domestic micro-CHP device. *Energy Convers Manag* (2020). https://doi.org/10.1016/j.enconman.2020.113429.

10. Damirchi H, Najafi G, Alizadehnia S, Mamat R, Nor Azwadi CS, Azmi WH, et al. Micro Combined Heat and Power to provide heat and electrical power using biomass and Gamma-type Stirling engine. *Appl Therm Eng* (2016). https://doi.org/10.1016/j.applthermaleng.2016.04.118.

11. Grosu L, Dobre C, Petrescu S. Study of a Stirling engine used for domestic micro-cogeneration. Thermodynamic analysis and experiment. *Int J Energy* Res (2015). https://doi.org/10.1002/er.3345.

12. Ferreira AC, Nunes ML, Teixeira JCF, Martins LASB, Teixeira SFCF. Thermodynamic and economic optimization of a solar-powered Stirling engine for micro-cogeneration purposes. *Energy* (2016). https://doi.org/10.1016/j.energy.2016.05.091.

13. Balcombe P, Rigby D, Azapagic A. Energy self-sufficiency, grid demand variability and consumer costs: Integrating solar PV, Stirling engine CHP and battery storage. *Appl Energy* (2015). https://doi.org/10.1016/j.apenergy.2015.06.017.

14. Zhang J, Cao S, Yu L, Zhou Y. Comparison of combined cooling, heating and power (CCHP) systems with different cooling modes based on energetic, environmental and economic criteria. *Energy Convers Manag* (2018). https://doi.org/10.1016/J.ENCONMAN.2018.01.019.

15. Ebrahimi M, Derakhshan E. Design and evaluation of a micro combined cooling, heating, and power system based on polymer exchange membrane fuel cell and thermoelectric cooler. *Energy Convers Manag* (2018). https://doi.org/10.1016/j.enconman.2018.06.007.

16. Balcombe P, Rigby D, Azapagic A. Environmental impacts of microgeneration: Integrating solar PV, Stirling engine CHP and battery storage. *Appl Energy* (2015). https://doi.org/10.1016/j.apenergy.2014.11.034.

17. UKERC Energy Data Centre. Electricity user load profiles by profile class (EDC0000041) (1997). https://ukerc.rl.ac.uk/DC/cgi-bin/edc_search.pl?GoButton=Detail&WantComp=42&WantResult=&WantText=EDC0000041 (accessed July 22, 2018).

18. IDAE. Domestic energy consumption. (2016).

19. Blaesser G, of the European Communities. Institute for Systems Engineering C, Informatics, Munro D. Guidelines for the Assessment of Photovoltaic Plants: Analysis and presentation of monitoring data. Document B. Office of Official Publications of the European Communities; (1995).